AGU PUBLICATIONS

JGR

Journal of Geophysical Research: Space Physics

RESEARCH ARTICLE
10.1002/2016JA023560

Key Points:
- We resolved the question that the Eureka thermospheric winds are larger than those of Resolute
- The TIEGCM simulation with Weimer ion convection overestimates the thermospheric winds in the polar cap
- The Weimer ion convection model also overestimates the zonal ion drift at Resolute

Correspondence to:
Q. Wu,
qwu@ucar.edu

Citation:
Wu, Q., G. Jee, C. Lee, J.-H. Kim, Y. H. Kim, W. Ward, and R. H. Varney (2017), First simultaneous multistation observations of the polar cap thermospheric winds, *J. Geophys. Res. Space Physics*, *122*, 907–915, doi:10.1002/2016JA023560.

Received 5 OCT 2016
Accepted 21 DEC 2016
Accepted article online 29 DEC 2016
Published online 11 JAN 2017

First simultaneous multistation observations of the polar cap thermospheric winds

Qian Wu[1], Geonhwa Jee[2], Changsup Lee[2], Jeong-Han Kim[2], Yong Ha Kim[3], William Ward[4], and Roger H. Varney[5]

[1]High Altitude Observatory, National Center for Atmospheric Research, Boulder, Colorado, USA, [2]Division of Polar Climate Change, Korea Polar Research Institute, Incheon, South Korea, [3]Department of Astronomy, Space Science, and Geology, Chungnam National University, Daejeon, South Korea, [4]Department of Physics, University of New Brunswick, Fredericton, New Brunswick, Canada, [5]Center for Geospace Studies, SRI international, Menlo Park, California, USA

Abstract Based on two northern (Eureka 80.0°N, 85.9°W, magnetic latitude (MLAT) 88, and Resolute 74.7°N, 94.8°W, MLAT 83) and one southern (Jang Bogo 74.7°S, 164.2°E, MLAT 77) polar cap stations, simultaneous thermospheric wind data during the northern (December) and southern (June) winter months were obtained and compared with the National Center for Atmospheric Research Thermosphere Ionosphere Electrodynamics General Circulation Model (TIEGCM) simulations driven by the Weimer ion convection model. The TIEGCM simulation overestimates the thermospheric wind by 30 to 60%. The thermospheric winds at Eureka were larger than those at Resolute probably because Eureka is at high-geomagnetic latitude. The observed ion drifts observed by Resolute Incoherent Scatter Radar North face at Resolute also show that the Weimer ion convection model overestimates the ion drift. The observation and simulation also appear to suggest that the ion convection pattern in the Weimer model may be too large. The observed thermospheric winds at Jang Bogo are smaller than the TIEGCM but mostly in the zonal component. The thermospheric winds are smaller at Jang Bogo than the two northern stations which are likely due to their lower magnetic latitude. The results indicate the presence of internal structure in the thermospheric winds inside the polar cap and call for more observations in the polar cap to be undertaken.

1. Introduction

High-latitude thermospheric winds are driven by pressure gradient forces and ion drag. The ion convection pattern has a strong impact on the thermospheric winds. At the same time, polar cap thermospheric winds can affect how the ionosphere respond to geomagnetic substorms by carrying disturbed ionosphere to mid-latitudes. For these reasons, it is important to have a good understanding of force driving the high-latitude thermospheric winds.

Over the years, there have been many high-latitude thermospheric wind observations from satellite-based Fabry-Perot interferometers (FPIs). On the ground, the FPI observations have been made in both northern and southern polar caps. In the Southern Hemisphere, high-latitude observations were made at South Pole (magnetic latitude (MLAT) 75) and Arrival Heights (MLAT 80) [e.g., *Hernandez and Roble*, 2003]. While Arrival Heights is inside the polar cap, South Pole is just poleward of the auroral oval. Hence, there was only single station observation of the southern polar cap thermospheric winds.

In the Northern Hemisphere, there have been prior FPI polar cap observations at Thule, Eureka, and Resolute [*Wu et al.*, 2008; *Won*, 1994; *Guo*, 2000; *Thayer et al.*, 1995]. However, there were no temporal overlaps between the three stations. These three stations have different geomagnetic latitudes, and whichever station was available at the time was used to represent the polar cap winds. However, as *Wu et al.* [2008] noted, the Eureka thermospheric winds were consistently larger than those from Thule and Resolute. Because the data were taken during different years, interpreting the apparent interstation difference was difficult since the reason could be spatial or interannual variations related to solar and geomagnetic activities.

The polar cap wind patterns can also be constructed based on satellite observations such as those from Dynamic Explorer 2 FPI, Upper Atmospheric Research Satellite Wind Imaging Interferometer, Challenging Minisatellite Payload, and Gravity field and steady-state Ocean Circulation Explorer accelerometers. These are statistical results derived from specific time periods, so there is little information on temporal variations.

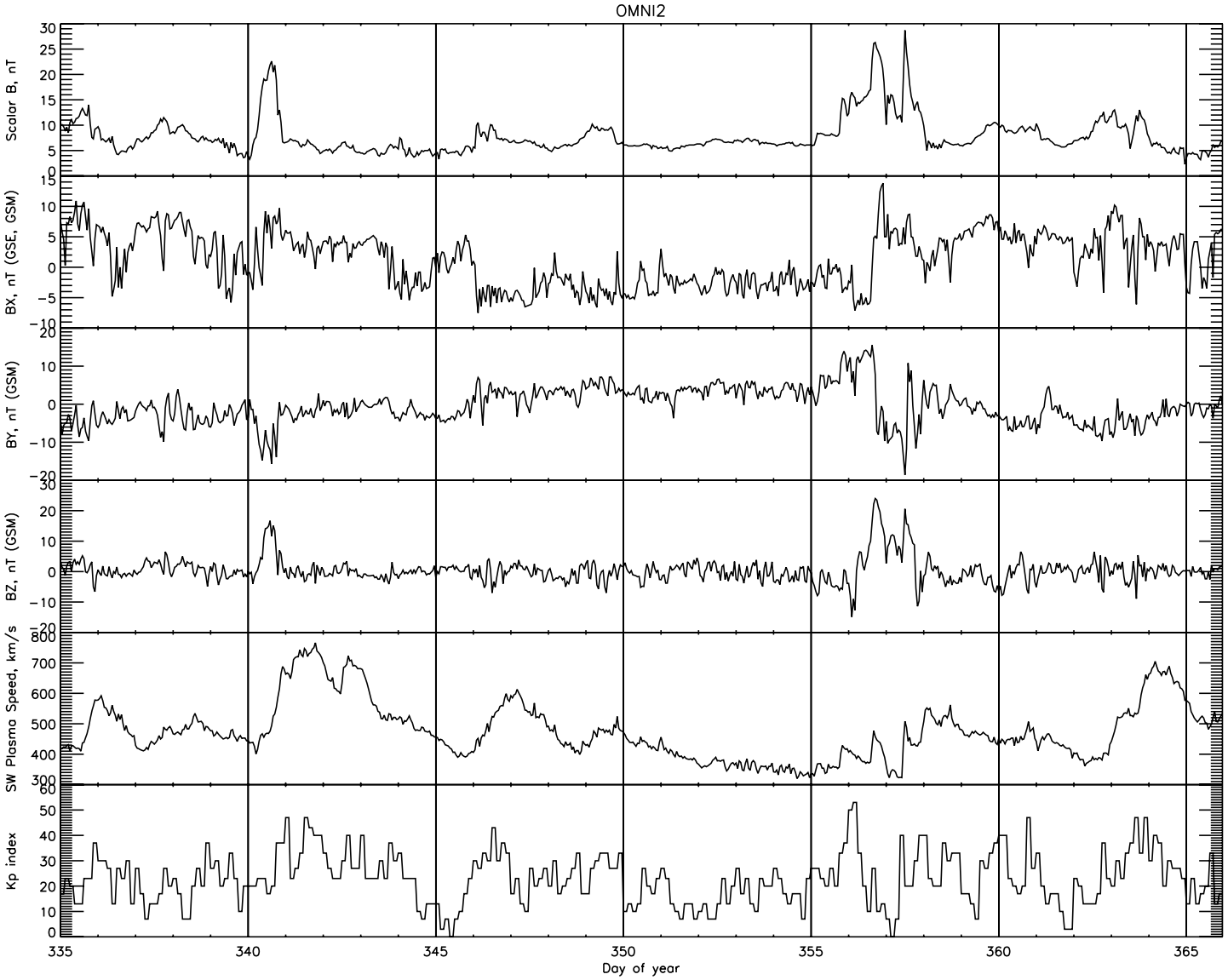

Figure 1. IMF parameters and *Kp* index (10X) for December 2014. The interplanetary magnetic field magnitude, B_x, B_y, and B_z; solar wind speed; and *Kp* index (10X) from 1 to 31 December are plotted. The data are from NASA OMNI site with low resolution (hourly).

Ground-based stations can provide information on temporal variability, but more than one station is necessary to diagnose spatial variations across the polar cap.

Recently, a small 630 nm emission only FPI was deployed at Eureka (80.0°N, 85.9°W, MLAT 88) in November 2014. The multi-emission Resolute FPI (74.7°N, 94.8°W, MLAT 83) was also refurbished and restarted in November 2014. For the first time, two FPIs are operating inside the polar cap taking simultaneous measurements of the redline winds. These two instruments provide an opportunity to examine spatial variations inside the polar cap. In the Southern Hemisphere, a new FPI was deployed in Jang Bogo station (74.7°S, 164.2°E, MLAT 77, also in the polar cap), Antarctica, in early 2014.

In this paper, we present the December 2014 winter solstice thermospheric wind data from Eureka and Resolute and June 2014 austral winter solstice data from Jang Bogo station. One goal is to see if there are any interstation differences in the northern polar cap thermospheric winds. Another goal is to examine possible interhemisphere differences in the polar cap thermospheric winds. We have also taken advantage of the Resolute Incoherent Scatter Radar (RISR) facility to examine observations of the ion drift from Resolute in

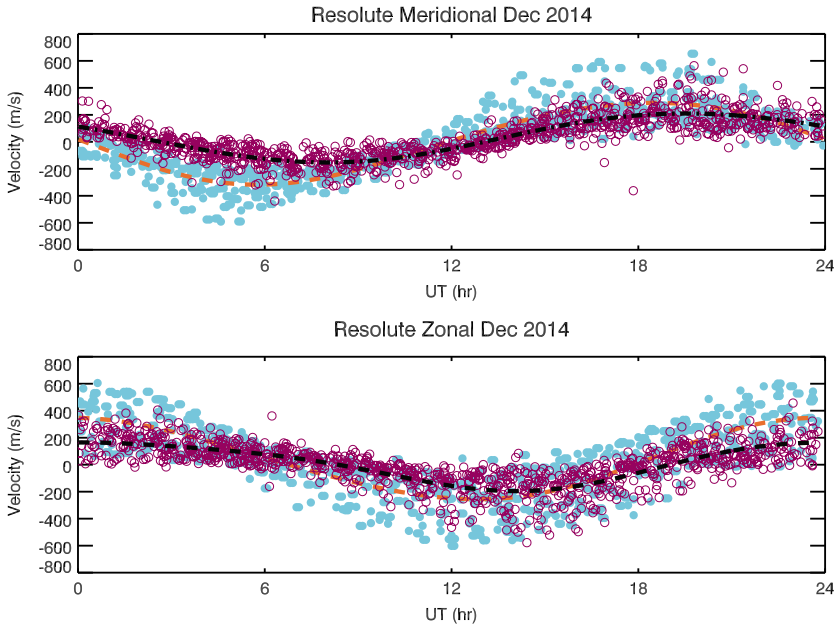

Figure 2. Resolute FPI observations and TIEGCM simulations. Resolute FPI thermospheric (top) meridional and (bottom) zonal winds. The FPI data are plotted with purple circles, and the diurnal and semidiurnal oscillations fit to the FPI data are plotted as a black dashed line. The TIEGCM simulation of the Resolute thermospheric winds is plotted as filled blue dots. The diurnal and semidiurnal fits to the TIEGCM simulations are plotted as an orange dashed line. The local midnight is at 06:00 UT and noon at 18:00 UT.

December 2014 in conjunction with the neutral wind observation. To understand the observations, they are compared with the National Center for Atmospheric Research (NCAR) Thermosphere Ionosphere Electrodynamics General Circulation Model (TIEGCM) based on *Weimer* [2005] ion convection models. The thermospheric and ionospheric observations can help validate the TIEGCM simulations.

2. Instruments

2.1. FPI

The FPI instrument at Resolute was initially deployed in 2003 and was described in *Wu et al.* [2004]. It has a 10 cm clear aperture etalon with a 2 cm gap. It was recently upgraded with a Princeton CCD camera and a new sky scanner. It samples the redline emission with 5 min integration time at four cardinal and the vertical directions.

The FPI at Jang Bogo has the same specifications as the one in Resolute. The FPI at Eureka has a 5 cm clear aperture etalon. It has a single rotating mirror and points to four cardinal directions at 45° elevation angle with a 700 s exposure time in each direction. The wind errors for the FPIs are on the order of few meters per second and vary with the redline emission intensity. All FPIs have cloud detector monitoring the sky conditions. Only the data taken during clear sky were used in the analysis.

2.2. Resolute Incoherent Scatter Radar North Face

Resolute Incoherent Scatter Radar North face (RISR-N) is an Advanced Modular Incoherent Scatter Radar (AMISR) instrument that was installed in Resolute in 2009 [*Bahcivan et al.*, 2010; *Dahlgren et al.*, 2012]. AMISRs are electronically steerable phased array radars than can steer from pulse to pulse. The RISR-N data analyzed in this paper come from the Imaging 52 mode experiment that was operating from 15 to 22 December 2014, which coincides with the FPI data interval to be analyzed in this paper. This radar mode is optimized for the estimation of *F*-region parameters over the entire radar field of view. The mode uses 50 beam positions and uncoded long pulses on three independent frequency channels. The received autocorrelation functions are integrated for 3 min and fit for electron density, electron temperature, ion temperature, and line-of-sight (LOS) ion drift velocity in each beam in 24 km resolution range gates. The LOS ion drifts from

Table 1. Amplitude and Phase of Diurnal and Semidiurnal Variations

	Resolute Meridional FPI and TIEGCM	Resolute Zonal FPI and TIEGCM	Eureka Meridional FPI and TIEGCM	Eureka Zonal FPI and TIEGCM	Jang Bogo Meridional FPI and TIEGCM	Jang Bogo Zonal FPI and TIEGCM	Resolute Meridional RISR and TIEGCM	Resolute Zonal RISR And TIEGCM
Diurnal amplitude (m/s)	182.7, 304.0	173.8, 297.5	241.8, 302.1	223.8, 281.2	139.4, 150.9	128.1, 209.4	356.3, 398.9	214.7, 356.1
Diurnal phase (UT)	19.80, 18.10	1.54, 0.27	17.83, 17.17	23.90, 23.50	13.15, 13.24	7.62, 7.82	15.72, 14.84	22.22, 0.95
Semidiurnal amplitude (m/s)	8.5, 18.4	32.2, 20.8	11.82, 13.89	3.4, 10.4	7.7, 39.4	4.9, 24.7	112.4, 119.7	38.7, 92.6
Semidiurnal phase (UT)	4.05, 10.52	8.95, 9.79	8.36, 2.77	5.9, 0.5	8.67, 9.61	4.70, 7.87	1.20, 11.25	4.65, 5.84
Background wind (m/s)	36.7, 1.9	8.0, 43.4	38.9, 0.04	70.2, 15.7	17.9, 31.7	34.5, 21.2	53.7, 11.0	−149.2,−91.4

all 50 beams are then combined into vector velocity estimates as a function of corrected geomagnetic latitude by using a Bayesian estimation algorithm [*Heinselman and Nicolls*, 2008]. This algorithm assumes uniformity in the magnetic east-west direction across the radar field of view and that perpendicular $E \times B$ drifts map between altitudes along equipotential magnetic field lines.

3. Model

The TIEGCM is a self-consistent first principles thermosphere ionosphere model developed at NCAR [*Roble et al.*, 1988; *Richmond et al.*, 1992]. It provides thermospheric and ionospheric parameters: neutral wind, temperature, ion drift, temperature, and composition from 97 km to ~500 km. In this study, we used a $2.5 \times 2.5°$ resolution and at 97 km, the global scale wave model [*Hagan and Forbes*, 2002] as the lower boundary condition. The Weimer ion convection model [*Weimer*, 2005] was used in the simulation because we are interested in its performance. The Weimer model is based on the 5 min resolution interplanetary magnetic field (IMF) parameters. Only hourly data from the simulation were saved for analysis to reduce the size of the save files.

4. Observations and TIEGCM Comparisons

Figure 1 shows the IMF and *Kp* index (10X) for December 2014. The geomagnetic activity was low for most of the period. Only near days 341 and 342 (6 and 7 December) and days 356, 360, and 363 (21, 26, and 29 December) are the *Kp* values briefly above 4 (40 in the plot).

Figure 2 shows the Resolute FPI thermospheric wind data and the TIEGCM simulation at the same location during December 2014. The meridional wind FPI observation (purple circles) showed mostly a diurnal variation. Midnight is near 06:00 UT and noon near 18:00 UT. The diurnal variation of the thermospheric wind in the polar cap is primarily a manifestation of the antisunward wind in part driven by the day-to-night pressure gradient near the Sun terminator. At the same time, the polar cap thermospheric winds are also affected by the ion convection at the high latitudes. The TIEGCM simulation (blue dots) also displays a similar diurnal variation. However, the TIEGCM simulation showed larger diurnal variation with stronger southward (antisunward) winds near midnight.

The zonal winds are also predominantly diurnal with 90° phase offset from the meridional winds. The TIEGCM simulation shows larger diurnal variations. We performed least squares fits to both FPI observations and TIEGCM of the meridional and zonal winds with diurnal and semidiurnal oscillations and background winds. The least squares fit curves for observations (simulation) are shown as the black (orange) dashed line. The least squares fit parameters are listed in Table 1.

Figure 3 shows the Eureka FPI observation and TIEGCM simulation comparison. Local midnight is near 05:00 UT and noon

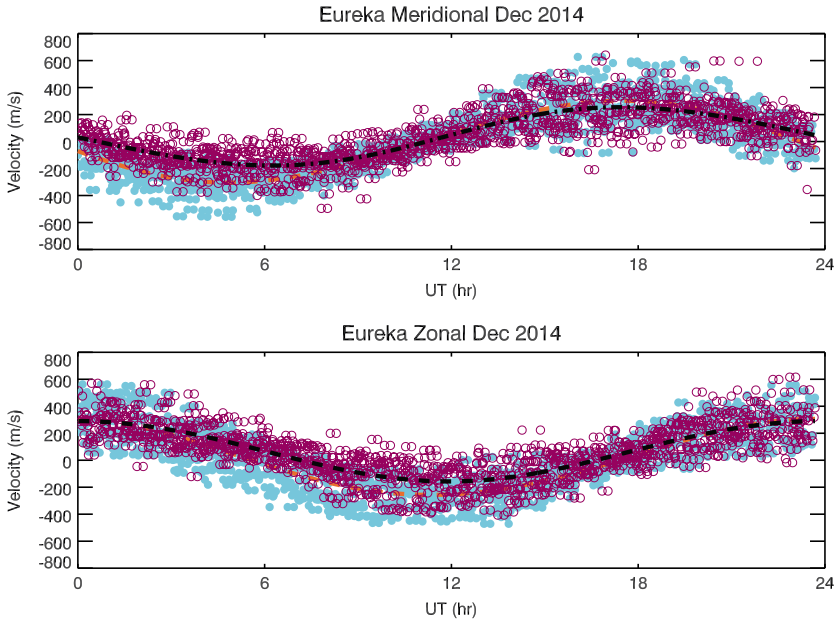

Figure 3. Eureka FPI observations and TIEGCM simulations. Same as Figure 2 but for Eureka. The Eureka local midnight is at 05:00 UT and noon at 17:00 UT.

close to 17:00 UT. Similar to the Resolute observations, both the FPI meridional and zonal winds have strong diurnal variations. The TIEGCM also exhibits stronger thermospheric winds compared to the FPI data. The least squares fit results are also shown in Table 1.

In the Southern Hemisphere the Jang Bogo station provided June 2014 observations. The IMF and geomagnetic *Kp* index (10X) are plotted in Figure 4. There are a few occasions when the *Kp* index was higher than 4 (days of year 159 and 170, 8 and 19 June). For the most part, the period of June 2014 was relatively quiet geomagnetically.

Figure 5 provides the comparison between the Jang Bogo FPI observations and the TIEGCM simulations. We should note that a negative meridional wind is poleward in the Southern Hemisphere. The local midnight is at 11:00 UT and local noon at 23:00 UT. The modeled and observed meridional winds are in good agreement with $<$10% difference in the diurnal variation amplitude (see Table 1). The TIEGCM zonal wind diurnal amplitude is 67% larger than the observations.

5. Discussion

5.1. FPI and Model Comparisons

It is apparent that in both the northern and southern polar caps, the TIEGCM overestimates the neutral wind diurnal variations. In the Northern Hemisphere, the difference is smaller at Eureka (25%) than at Resolute (50%). In the Southern Hemisphere the difference for meridional wind is 7% and zonal wind 65%. We should note that the magnetic latitudes of these stations vary. It is highest at Eureka (MLAT 88) followed by Resolute (MLAT 82) with Jang Bogo being the lowest (MLAT 77). The TIEGCM performs better near the magnetic pole, and as the stations get closer to the auroral oval, its performance degrades. The diurnal variation phase differences between the observations and simulations are small ($<$2 h).

The semidiurnal variation in the modeled results and observations was also calculated (see Table 1). The semidiurnal variation is likely related to the shape of the auroral oval. There are large discrepancies between the observations and simulations. Since the semidiurnal variations are secondary compared to the diurnal variation, some larger discrepancies are not unexpected. Overall, the TIEGCM is likely to overestimate the semidiurnal variations as well. *Wu et al.* [2008] also compared the TIEGCM simulations with the Resolute and Eureka FPI observation. The TIEGCM simulation in that study was driven by the Heelis model [*Heelis et al.*, 1982]. The TIEGCM and FPI differences in that case were even larger than in the current analysis.

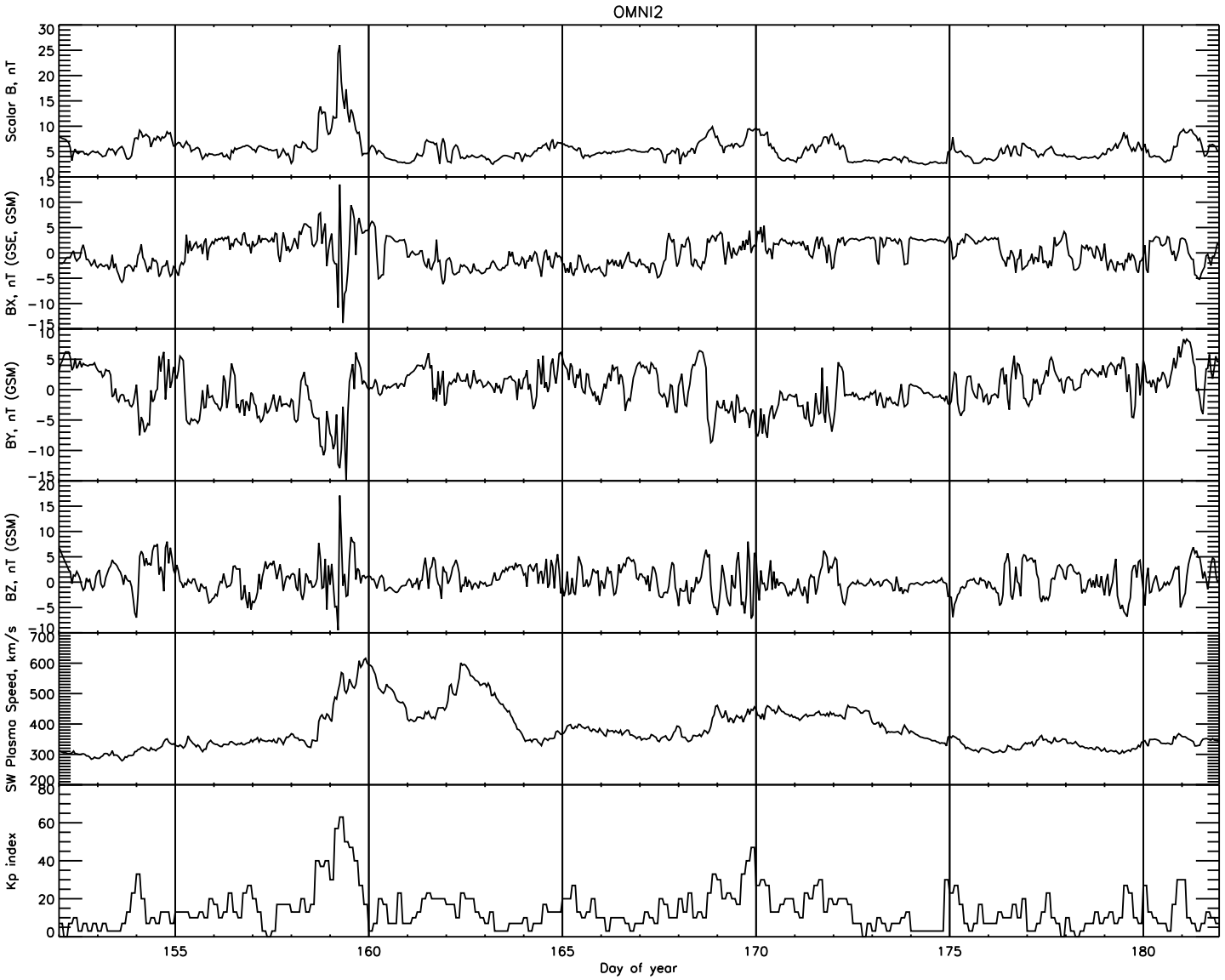

Figure 4. IMF parameters and *Kp* index (10X) for June 2014. Same as Figure 1 but for June 2014.

That is consistent with the *Wu et al.* [2015] study, which compared the Heelis and Weimer models. *Wu et al.* [2015] noted that the Heelis model tends to give larger winds than the Weimer model in the polar cap. This study shows that even Weimer model tends to overestimate the thermospheric wind diurnal variations in the polar cap.

5.2. RISR and Weimer Comparisons

To examine the cause of the TIEGCM overestimation of the polar cap winds, the Weimer ion convection ion drift velocity is compared with the RISR-N (Resolute Incoherent Scatter Radar North face) data during December 2014 (see Figure 6). Both the RISR-N and TIEGCM (Weimer convection) ion drift data are plotted. Since the TIEGCM simulation has only hourly data, the model data are plotted as a set of horizontal bars. This is in contrast to the high temporal resolution RISR-N data. We performed the same least squares fitting to the observations and TIEGCM simulations. The fitting results are also listed in Table 1. The TIEGCM slightly overestimates the diurnal variation in the meridional direction (10%) while greatly overestimates the ion drift in the zonal direction (68%). The large zonal ion drift tends to appear near dawn and dusk. *Wu et al.* [2015] compared the Weimer and Super Dual Auroral Radar Network (SuperDARN)-based convection at high

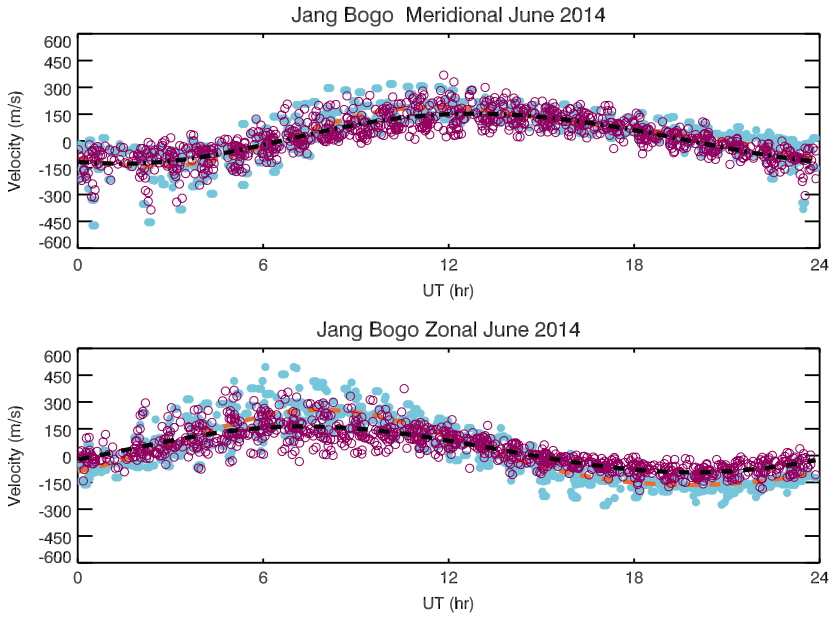

Figure 5. Jang Bogo FPI observations and TIEGCM simulations. Same as Figure 2 but for Jang Bogo. The Jang Bogo local midnight is at 11:00 UT and noon at 23:00 UT.

latitudes and noted that the Weimer model cross polar cap potential is larger than that based on the SuperDARN data. The convection pattern from Weimer is also larger. A larger convection pattern means that within that area the prevailing winds will be mostly antisunward, which corresponds to the diurnal variation in the ground-based observed thermospheric winds. The size of the convection pattern would change the winds. The changes near the magnetic pole will be smaller. The winds further away from the pole near the edge of the polar cap will be more affected. This seems to be consistent with the model and observation comparisons, for which the discrepancies are larger further away from the magnetic pole and the model overestimates the winds.

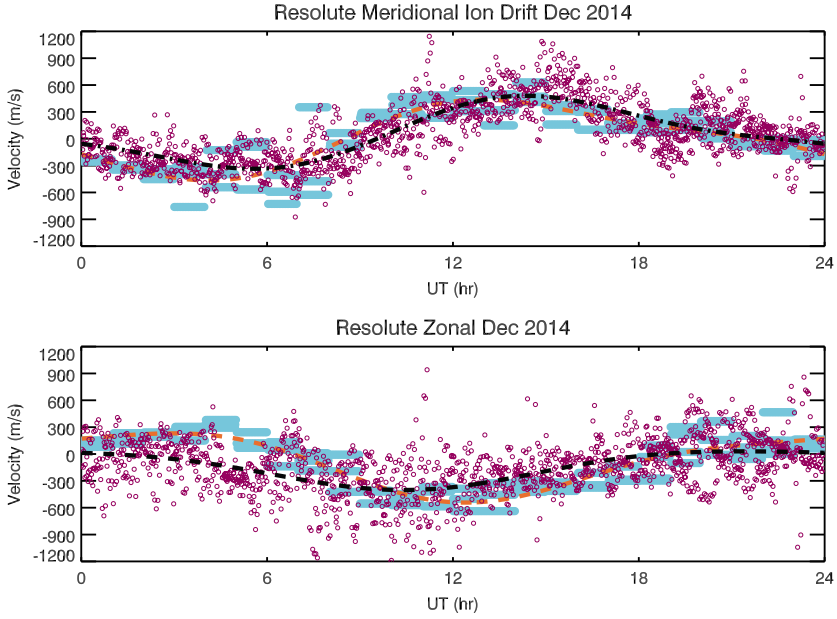

Figure 6. RISR and TIEGCM Weimer comparison. Same as Figure 2 but for Resolute RISR-N data and TIEGCM *Weimer* [2005] ion drift output. The data covers from 15 to 22 December with Imaging 52 mode. For each of the RISR data point, TIEGCM ion drift data are plotted at the UT. Since the TIEGCM output is hourly, the TIEGCM data look like horizontal bars.

5.3. Resolute and Eureka Comparisons

Wu et al. [2008] noted that the Eureka thermospheric winds are larger than those from Resolute by ~60%. However, because the data sets from the two stations were taken during different years, it was impossible to distinguish whether this difference was interstation or due to interannual variations. The simultaneous observations from the two stations reported here resolve this question. The observed diurnal variations in the thermospheric winds from Eureka are larger than those from Resolute by ~30% as shown in Table 1. The simulated results showed much smaller differences between the two stations. This could be indicative that the Weimer model has a larger polar cap with a more uniform wind field. The observations seem to suggest that the convection pattern may be smaller than the Weimer model predicts.

5.4. Interhemispheric Comparisons

The thermospheric winds at Jang Bogo are smaller than those at Resolute and Eureka. There could be interhemispheric differences involved. But, the Jang Bogo geomagnetic latitude is lower than the other two northern stations. We have shown that thermospheric winds at Resolute are smaller than those at Eureka, probably because the magnetic latitude at Resolute is lower than that of Eureka. Since the magnetic latitude of Jang Bogo is even lower, we may expect even smaller thermospheric winds. Both the model and observations indicate that the Jang Bogo thermospheric wind should be smaller. The north-south differences in the thermospheric winds are more likely due to the geomagnetic latitudinal difference. This question will not be resolved until we have more stations in Antarctica with similar latitudes as Resolute and Eureka in order to have a better estimate of the interhemispheric differences.

5.5. Ion and Neutral Velocity Differences

At Resolute, we have both the neutral and ion velocity measurements and simulations. The ion drift diurnal variations observed with RISR are larger than those deduced from the observed thermospheric wind by 95% in the meridional and 25% in the zonal component. The simulated ion drift and thermospheric winds have smaller differences (30% in meridional and 20% in zonal). The neutral winds at Resolute are not entirely determined by the local ion drifts. The neutrals interacted with ions long before they reach Resolute. The meridional winds are mostly from the dayside and midnight sectors of the polar cap, where the meridional winds are largest. The large difference between the ions and neutrals in the observations seems to imply that neutrals were not accelerated by the ions much in the real world. The small differences in the simulations, on the other hand, suggest that the neutrals have been accelerated by ion drag for a while in the model. We should note that the observed ion drifts by RISR-N have large variabilities, while the Weimer ion convection model outputs are much smoother. The smooth output from the Weimer model may provide more persistent forcing to the neutrals than the highly variably real ion drifts, which may not drag the neutrals in a consistent way. The highly variably ion drifts may also imply that there may be more Joule heating in the polar cap, because Joule heating is proportional to the square of the ion drift and neutral wind differences. While the neutral wind tends to have slower variations, highly variable ion drift can introduce and maintain larger differences between the ion and neutral speeds causing larger Joule heating in the polar cap as reported recently [e.g., *Huang et al.*, 2016].

6. Summary

We present the first simultaneous multistation observations of polar cap thermospheric winds. We found that the Eureka thermospheric winds are larger than those at Resolute. The TIEGCM simulation with Weimer ion convection overestimates the thermospheric winds in the polar cap particularly at places away from the magnetic pole. The zonal winds have large differences. The Weimer ion convection model also overestimates the zonal ion drift at Resolute as compared to the RISR-N. The data model comparison suggests that the Weimer ion convection pattern may be too large.

Acknowledgments
The work by Q.W. is supported by NSF grant AGS1339918 and NASA grant NNX13AF93G. This work is also supported by the grant PE17020 at Korea Polar Research Institute. The TIEGCM is available from NCAR HAO website. The RISR and FPI data are available upon request. NCAR is supported by the National Science Foundation. The authors acknowledge the contribution from the High Altitude Observatory Instrument Group in instrument construction. RISR-N is operated by SRI International under NSF cooperative agreement AGS-1133009. The work of W.E.W. is supported through the Geospace Observatory program of the Canadian Space Agency and a Discovery grant provided by the Natural Science and Engineering Research Council.

References

Bahcivan, H., R. Tsunoda, M. Nicolls, and C. Heinselman (2010), Initial ionospheric observations made by the new Resolute Incoherent Scatter Radar and comparison to solar wind IMF, *Geophys. Res. Lett.*, *37*, L15103, doi:10.1029/2010GL043532.

Dahlgren, H., J. L. Semeter, K. Hosokawa, M. J. Nicolls, T. W. Butler, M. G. Johnsen, K. Shiokawa, and C. Heinselman (2012), Direct three-dimensional imaging of polar ionospheric structures with the Resolute Bay Incoherent Scatter Radar, *Geophys. Res. Lett.*, *39*, L05104, doi:10.1029/2012GL050895.

Guo, W. (2000), F-region winds over the central polar cap, PhD thesis, Univ. of Saskatchewan, Saskatoon.
Hagan, M. E., and J. M. Forbes (2002), Migrating and nonmigrating tides in the middle and upper atmosphere excited by latent heat releases, *J. Geophys. Res.*, *107*(D24), 4754, doi:10.1029/2001JD001236.
Heelis, R. A., J. K. Lowell, and R. W. Spiro (1982), A model of the high latitude ionosphere convection pattern, *J. Geophys. Res.*, *87*, 6339–6345, doi:10.1029/JA087iA08p06339.
Heinselman, C. J., and M. J. Nicolls (2008), A Bayesian approach to electric field and E-region neutral wind estimation with the Poker Flat Advanced Modular Incoherent Scatter Radar, *Radio Sci.*, *43*(5), 1–15, doi:10.1029/2007RS003805.
Hernandez, G. and R. G. Roble (2003), Simultaneous thermospheric observations during the geomagnetic storm of April 2002 from South Pole and arrival heights, Antarctica, *Geophys. Res. Lett.*, *30*(10), 1511, doi:10.1029/2003GL016878.
Huang, Y., Q. Wu, C. Y. Huang, and Y.-J. Su (2016), Thermosphere variation at different altitudes over the northern polar cap during magnetic storms, *J. Atmos. Sol. Terr. Phys.*, *146*, 140–148, doi:10.1016/j.jastp.2016.06.003.
Richmond, A. D., E. C. Ridley, and R. G. Roble (1992), A thermosphere/ionosphere general circulation model with coupled electrodynamics, *Geophys. Res. Lett.*, *19*, 601–604, doi:10.1029/92GL00401.
Roble, R. G., E. C. Ridley, and A. D. Richmond (1988), A coupled thermosphere/ionosphere general circulation model, *Geophys. Res. Lett.*, *15*, 1325–1328, doi:10.1029/GL015i012p01325.
Thayer, J. P., G. Crowley, R. J. Niciejewski, T. L. Killeen, J. Buchau, and B. W. Reinisch (1995), Ground-based observations of ion/neutral coupling at Thule and Qanaq, Greenland, *J. Geophys. Res.*, *100*, 12,189–12,199, doi:10.1029/95JA00131.
Weimer, D. R. (2005), Improved ionospheric electrodynamic models and application to calculating Joule heating rates, *J. Geophys. Res.*, *110*, A05306, doi:10.1029/2004JA010884.
Won, Y.-L. (1994), Studies of thermospheric neutral winds utilizing ground-based optical and radar measurements, PhD thesis, Univ. of Michigan, Ann Arbor.
Wu, Q., R. D. Gablehouse, S. C. Solomon, T. L. Killeen, and C.-Y. She (2004), A new NCAR Fabry-Perot Interferometer for upper atmospheric Research, *Proc. SPIE*, *5660*, 218–227.
Wu, Q., D. McEwen, W. Guo, R. J. Niciejewski, R. G. Roble, and Y.-I. Won (2008), Long-term thermospheric neutral wind observations over the northern polar cap, *J. Atmos. Sol. Terr. Phys.*, *70*, 2014–2030, doi:10.1016/j.jastp.2008.09.004.
Wu, Q., B. A. Emery, S. G. Shepherd, J. M. Ruohoniemi, N. A. Frissell, and J. Semeter (2015), High-latitude thermospheric wind observations and simulations with SuperDARN data driven NCAR TIEGC M during the December 2006 magnetic storm, *J. Geophys. Res. Space Physics*, *120*, 6021–6028, doi:10.1002/2015JA021026.